PRE-PRINT of the article "Blocken B, Stathopoulos T, Carmeliet J. 2008. Wind environmental conditions in passages between two long narrow perpendicular buildings. **Journal of Aerospace Engineering – ASCE** 21(4): 280-287".

Wind environmental conditions in passages between two long narrow perpendicular buildings

B. Blocken*[1], T. Stathopoulos[2], F.ASCE, J. Carmeliet[3,4]

* Corresponding author

Abstract

This paper presents wind tunnel measurements of pedestrian wind conditions in passages between various configurations of two long narrow perpendicular buildings in open country exposure. The investigated parameters are passage width, building height and wind direction. The measurements were made along the passage centerline. The aim of the paper is to provide more insight in the pedestrian wind conditions in these basic building configurations, to address some contradictory statements reported in the literature and to provide detailed experimental data for Computational Fluid Dynamics (CFD) validation. The results show that the wind speed amplification factors in diverging passages are generally larger than in converging passages. It is also shown that the maximum wind speed amplification factors increase monotonically with decreasing passage width, contrary to some general building design guidelines proposed in the past for such building configurations. Significant issues concerning the use of the experimental data for CFD validation are also discussed.

Subject headings: Wind tunnel test; Boundary layer flow; Turbulent flow; Buildings; Wind speed; Amplification; Computational Fluid Dynamics.

[1] Assistant professor, Building Physics and Systems, Technische Universiteit Eindhoven, P.O. box 513, 5600 MB Eindhoven, The Netherlands, b.j.e.blocken@tue.nl, Tel. +31 40 247 2138, Fax +31 40 243 8595

[2] Professor, Centre for Building Studies, Department of Building, Civil and Environmental Engineering, Concordia University, 1455 de Maisonneuve Blvd West, H3G 1M8, Montreal, Quebec, Canada, statho@bcee.concordia.ca

[3] Professor, Chair of Building Physics, Swiss Federal Institute of Technology ETHZ, ETH-Hönggerberg, CH-8093 Zürich, Switzerland and, Empa, Swiss Federal Laboratories for Materials Testing and Research Laboratory for Building Technologies, Überlandstrasse 129, CH-8600 Dübendorf, Switzerland. E-mail: carmeliet@arch.ethz.ch

Introduction

Urban aerodynamics research, as part of Aerospace Engineering, is recognized as becoming increasingly important to ensure the quality of human life in outdoor urban environments (ASCE 2003, Mallah 2006, Stathopoulos 2006). It is essential to understand a variety of urban problems ranging from pedestrian wind nuisance around buildings (ASCE 2003, Stathopoulos 2006) over pollutant dispersion (Meroney 2004) to wind-driven rain exposure of building facades (Blocken and Carmeliet 2004). Wind tunnel modelling and Computational Fluid Dynamics (CFD) are recognized as the main tools for research in urban aerodynamics (ASCE 2003, Mallah 2006, Stathopoulos 2006). However, since the application of Direct Numerical Simulation (DNS) to practical engineering problems will not be feasible in the foreseeable future, the application of CFD with turbulence models still requires validation by accurate and detailed wind tunnel measurements (Stathopoulos 2002, ASCE 2003). Validation studies are often performed on generic or sub-configurations of more complex real configurations. In case of urban aerodynamics, examples of sub-configurations of real urban environments are isolated low-rise and high-rise buildings, passages between buildings, passages through buildings, etc. One of the most common of these sub-configurations is a passage between two buildings.

Passages between buildings can be responsible for increased wind speed and wind nuisance at pedestrian level (Ishizaki and Sung 1971, Wiren 1975, Lawson 1980, Beranek 1982, Stathopoulos and Storms 1986, Stathopoulos et al. 1992, Stathopoulos and Wu 1995, To and Lam 1995, ASCE 2003, Blocken et al. 2004, 2007a, Stathopoulos 2006). Different categories of passages between buildings can be distinguished, some of which are indicated in Fig. 1: (1) passages between parallel buildings placed side-by-side; (2) passages between parallel shifted buildings; and (3) passages between perpendicular buildings. This paper focuses on passages between perpendicular buildings. Depending on the wind direction, this type of passage can be called “converging passage” or “diverging passage”. A distinction can also be made between two types of studies concerning wind conditions in passages: (1) fundamental studies, which are typically conducted for simple, generic building configurations as indicated in Fig. 1, to provide insight in the flow behavior, for parametric analyses and for CFD validation; and (2) applied studies for more complex building configurations. This paper will be limited to generic building configurations with only two buildings.

Many fundamental studies of wind conditions in passages between buildings have been conducted in the past, by wind tunnel modeling and by numerical simulation with CFD. The majority of these studies focused on passages between parallel buildings. Pedestrian wind conditions in passages between non-parallel buildings have received much less attention. Wiren (1975) performed wind tunnel experiments for perpendicular buildings and for various wind directions (converging and diverging passages). Gandemer (1975) and Lawson (1980) reported wind tunnel results for converging passages. Beranek (1982) performed sand-erosion tests to compare the pedestrian wind conditions in perpendicular converging versus diverging building arrangements. However, the conclusions of previous studies also show some contradictions. The results by Wiren (1975) for a narrow passage (w = 4 m) between two long narrow buildings (L = 60 to 80 m; B = 12 m) with various passage width-to-height ratios (w/H = 0.17, 0.22, 0.33, 0.67 for H = 24, 18, 12, 6 m, respectively) indicate that the wind speed amplification factors in the passage at pedestrian level increase with decreasing w/H. The wind speed amplification factor U/U_0 is defined as the ratio of the local mean wind speed (U) to the mean wind speed that would occur at the same position but without the buildings present (U_0). Wiren’s experiments were conducted for open country exposure (power law exponent $\alpha = 0.125$). On the other hand, Gandemer (1975) states that for an open country exposure, for a total length of the two long buildings $2L > 100$ m and for $H > 15$ m, a maximum flow will go through a converging passage when w/H is about 2 or 3. Lawson (1980) seems to corroborate Gandemer’s statements by mentioning that little acceleration occurs in the passage when the ratio w/H is outside the interval [0.5; 4]. The results and statements by Gandemer (1975) and Lawson (1980) however seem to contradict the results by Beranek that show monotonically increasing amplification factors for long narrow buildings (L = 80 m, B = 10 m), when the ratio w/H decreases from 1 to 0.25 (H = 25, 50 m). These apparent contradictions can not be analyzed in detail because these authors, except for Wiren (1975), did not report the details of their experiments. In addition, some

parameters were different. Wiren (1975) performed experiments for open country exposure ($\alpha = 0.125$), while Beranek used urban exposure ($\alpha = 0.28$). Furthermore it is not clear whether "maximum flow" in Gandemer (1975) and Lawson (1980) refers to a maximum flux of air through the passage or to maximum amplification factors at pedestrian level. The latter seems to be more likely, since pedestrian-level winds were the focus of the reports by both authors and because they both specifically referred to values at pedestrian height.

Due to the limited number of wind tunnel experiments available, the lack of knowledge concerning the experimental conditions and the generally small number of measurement positions in these experiments, little is known about the wind speed conditions in converging and diverging passages. This paper reports detailed wind tunnel measurement results for a variety of configurations of two long narrow perpendicular buildings with different passage widths (w/H ranging from 0.17 to 3). The aim of the study is (1) to provide more insight in the pedestrian wind conditions for these basic building configurations; (2) to address the above-mentioned previous contradictory conclusions; and (3) to provide detailed experimental data for CFD validation. First, the experimental conditions are described. Next, the experimental results are presented and analyzed. Finally, the use of the experimental data for CFD validation is discussed.

Experimental conditions

The measurements were conducted at a scale of 1:400 in the boundary layer wind tunnel of the Building Aerodynamics Laboratory at Concordia University (Stathopoulos 1984). The basic building configuration and building dimensions are illustrated in Fig. 2, where r is a dimensionless coordinate along the passage centerline with r = 0 at the location of the narrowest passage opening. The unit length of r is $L\sqrt{2}/2$. The direction of the r-axis is according to the flow direction (positive in downstream direction). The building dimensions and experimental conditions were taken according to Gandemer (1975): H > 15 m, 2L > 100 m and open country exposure. Before the actual measurements, the behavior of the simulated atmospheric boundary layer (ABL) in the empty wind tunnel (with roughness elements but without the two building models) was analyzed. The incident profiles (at r = 0) were recorded (Fig. 3a), and the change of the boundary layer over the turntable at pedestrian height (5 mm; 2 m in full scale) was measured (Fig. 3b). These aspects can be quite important for CFD validation as shown earlier (Blocken et al. 2007a, 2007b). Figure 3a illustrates the profiles along the bottom half of the wind tunnel height. In this figure, U_g denotes the wind speed at gradient height. The measured incident mean wind speed profile resembled a power-law function with exponent $\alpha = 0.125$. The reference incident wind speed U_0, taken at 5 mm height (pedestrian-level; 2 m in full scale) and at r = 0, was 7.4 m/s. The turbulence intensity of the incident flow, based on the local mean wind speed, ranged from 12 % at 5 mm height to 2 % at gradient height (0.75 m model scale; 300 m full scale). Figure 3b shows that the pedestrian-level change in mean wind speed over the turntable (between r = -2 and r = 2) is 10 %, while the turbulence intensity decreases by 36 %. Note that the distance between r = -2 and r = 2 corresponds to 707 mm (model scale; 283 m in full scale). U_0 and I_0 refer to the values at r = 0. Note that these changes would be even more important for higher power law exponents and that they should be accurately reproduced when using these data for CFD validation.

For all building configurations the blockage ratio was lower than 1%. The building Reynolds number $Re_b = 17{,}000$, which is above the minimum value of 11,000 for Reynolds-number independent flow as stated by Snyder (1981). Wind speed and turbulence intensity measurements were made with a TSI hot-wire anemometer at pedestrian height and at nine positions along the passage centerline: r = -1, -0.5, -0.25, -0.125, 0, 0.125, 0.25, 0.5, 1. The probe with a single oriented hot wire was positioned so that the wire was horizontal and perpendicular to the passage centerline. Hot-wire measurements tend to overestimate the mean wind speed and underestimate the turbulent fluctuations in highly turbulent flows because of the well-known turbulence error (Cook and Redfearn 1976, Bottema 1993). The errors become more pronounced as turbulence intensity increases, and measurements are considered inaccurate when the turbulence intensity exceeds 30% ($I/I_0 > 2.5$). Because the present study mainly focuses on the amplification factors near r = 0 (Fig. 2), where mean wind speed is high and turbulence intensity is low, the single oriented hot wire was

considered suitable. Another systematic error can be introduced by oblique incidence of the flow on the hot wire. Most measurements were conducted with the upstream, undisturbed wind direction parallel to the passage centerline ($\theta = 0°$) (Fig. 2) and therefore perpendicular to the hot wire. However, when $\theta \neq 0°$, the angle φ between the local horizontal wind velocity component and the normal to the wire is likely to be also different from zero and errors are introduced. These errors were measured for the hot-wire probe placed in the simulated atmospheric boundary layer at pedestrian height, in absence of the buildings. For the ratio U/U_0, they are -2, -4, -17 and -22% for $\varphi = 15$, 30, 45 and 60° respectively. For the ratio I/I_0, these values are 0, -4, -4 and -7% for the same wind direction values. Because the local wind directions φ at the measurement positions were not known, no corrections could be made and the uncorrected results are presented in this paper.

Experimental results and analysis

The measurement results are presented as amplification factors for the mean wind speed (U/U_0) and turbulence intensity (I/I_0) along the passage centerline at pedestrian height, where the reference values U_0 and I_0 are always taken without the buildings present and at $r = 0$. In the first three subsections, the results for wind direction $\theta = 0°$ are analyzed. In the last subsection, the influence of wind direction is discussed.

Converging building arrangements ($\theta = 0°$)

Figure 4a illustrates U/U_0 along the passage centerline between r = -1 and 1, for the converging building arrangement with H = 30 m and with the passage width as a parameter. The maximum value is found for the narrowest passage (w = 10 m; $U/U_0 = 1.15$) and it decreases as the passage width increases. Its location moves downstream as the passage becomes wider. For all passage widths investigated here, U/U_0 is smaller than one along the largest part of the passage centerline, indicating that the buildings provide shelter to these locations from the wind. This is more pronounced in the upstream region (r = -1 to -0.25) than in the downstream region (r = 0.25 to 1). Figure 4b displays I/I_0, which is related to U/U_0. The minimum value occurs at r = 0 or just downstream of this position. For the narrowest passage widths, a strong increase in the upstream and downstream region is observed, where the local turbulence intensity can exceed 30% ($I/I_0 > 2.5$), compromising hot-wire measurement accuracy. Because of the strong relation between U/U_0 and I/I_0, the discussion in the remainder of this paper will focus on U/U_0, but all figures for I/I_0 will be provided. Figure 5a shows the results for H = 60 m. The maximum value (w = 10 m; $U/U_0 = 1.53$) is clearly larger than for H = 30 m. For the narrower passage widths also the upstream flow deceleration is more pronounced for H = 60 m. For w = 10, 30 and 50 m, the location of the maxima hardly changes with increasing building height. Both Figure 4a and 5a indicate that, at least for the narrower passage widths, there is a considerable slowdown of the wind in the upstream part of the passage ($r < 0$) (wind-blocking effect; Blocken and Carmeliet 2006, 2007a), and this effect extends for a considerable distance upstream. From this slowly moving mass of air, a jet emerges in the narrowest part of the passage ($r = 0$) that subsequently decays quite rapidly ($r > 0$) due to momentum exchange with the flow in the wake of the two buildings.

Diverging building arrangements ($\theta = 0°$)

Figure 6a displays U/U_0 for the diverging arrangement with H = 30 m. Contrary to the converging arrangement with H = 30 m, the maximum values are quite high (w = 10 m; $U/U_0 = 1.47$), and the upstream decrease of U/U_0 is somewhat less pronounced and concentrated at a location closer to $r = 0$. As for the converging arrangement, the maximum value decreases and its location moves further downstream with increasing passage width. Comparing Figures 6a and 7a it is observed that the maximum U/U_0 for the narrowest passage widths is almost the same for H = 30 m and H = 60 m: for w = 10 m, $U/U_0 = 1.47$ and 1.49, respectively, and for w = 30 m, $U/U_0 = 1.43$ and 1.45, respectively. For these passage widths, the location of the maxima also remains fixed at approximately the same position for H = 30 and H = 60 m. Both Figures 6a and 7a indicate that, at least for the narrower passage widths, there is a slowdown of the wind in the upstream region ($r < 0$) (wind-blocking effect) but its extent is considerably less than for

the converging building arrangements. This is logical because the diverging shape of the buildings does not "catch" the wind, as opposed to the converging arrangement. Also here, a jet exists in the passage that originates from the two corner streams at the upstream building corners (r = 0) and it rapidly decays in the wake of the buildings (r > 0) due to jet entrainment.

Variation of amplification factors with w/H (θ = 0°)

Figure 8 presents a summary of the results for wind direction θ = 0°, for all passage widths and building heights investigated. Figure 8a illustrates U/U_0 at r = 0, as a function of the ratio w/H, for both the converging and the diverging building arrangements. For H = 30 m and for all passage widths investigated, U/U_0 for the diverging arrangement is considerably larger than for the converging arrangement. For H = 60 m, a similar conclusion holds when w/H > 0.5. Below this value, U/U_0 in the converging passage clearly becomes very large and rises above the value in the diverging passage. Figure 8b displays the maximum U/U_0 along the passage centerline between r = -1 and r = 1, $(U/U_0)_{max}$, as a function of w/H. These values are always larger than those in Fig. 8a, but they lead to similar conclusions. Note that the curves for the diverging arrangements are about the same for both building heights, while those for the converging arrangement show a strong dependence on building height.

The fact that the wind speed amplification factors are generally larger for the diverging than for the converging arrangements is opposite to what one might assume. The increased wind speed amplification factors in a converging arrangement are sometimes attributed to the Venturi-effect (Gandemer 1975, Lawson 1980) and this might lead to the expectation that they would be less pronounced for a diverging arrangement. The Venturi-effect refers to the inverse proportionality between the fluid speed and the cross-section through which the flow passes. Because this strictly only applies to confined flows, the use of this terminology is considered less appropriate for the non-confined flows in urban aerodynamics. The observation that the amplification factors for the diverging arrangement are generally larger than those for the converging arrangement can be explained by the wind-blocking effect rather than by the Venturi-effect. The wind-blocking effect has been investigated earlier for the case of passages between parallel buildings (Blocken et al. 2007a). It refers to the slow-down of wind speed upstream of the buildings. This effect is more pronounced for the converging arrangements that "catch" the wind and significantly slow down a large mass of air over quite a large distance upstream of the passage at r = 0. This will cause part of this air mass to flow around and especially over the passage, rather then being forced through the narrowest passage opening.

The wind-blocking effect might also explain the specific flow behavior shown in Figure 8b. It could be argued that for the diverging arrangement, because the wind-blocking effect is less pronounced, most air will flow around and through the passage, and relatively little air will flow over the buildings. As such, the flow around the diverging building arrangement shows to some extent a 2D behavior (flow with relatively small vertical velocity components). Therefore, $(U/U_0)_{max}$ for the diverging arrangement is almost identical for H = 30 and 60 m, for all passage widths. For the converging arrangement, the wind-blocking effect is much more pronounced. For H = 30 m, it will force a large part of the approaching wind to flow not only around but also over the buildings, which yields lower values for $(U/U_0)_{max}$. For H = 60 m, the larger building height provides a larger resistance to the flow over the buildings, and as a result more air will go around the buildings and through the passage. This might explain why $(U/U_0)_{max}$ is larger for H = 60 m than for H = 30 m.

The findings for the converging building arrangements from the present wind tunnel results, presented as (U/U_0) versus w/H in Figure 8, can be compared to those from previous studies. The present results seem to corroborate the findings by Wiren (1975) and Beranek (1982), but they do not seem to correspond to those by Gandemer (1975) and Lawson (1980) because they show that $(U/U_0)_{max}$ increases monotonically with decreasing w/H. Also U/U_0 values at r = 0 seem to increase with decreasing w/H. Contrary to some previous studies' results, no clear local maxima are found for w/H between 2 and 3 or between 0.5 and 4. Instead, the maxima for the converging arrangements are found for w/H < 0.5. The reason for these contradictory findings is not clear, especially since the study in this paper was conducted for exactly the same conditions set forth by Gandemer for the occurrence of the "Venturi-effect". A

possible reason could be that their tests were conducted for buildings that are not perpendicular, although this could not be verified. Regardless, the present measurements indicate that previous conclusions may not be valid for all perpendicular building configurations. This is significant because these previous conclusions have been made available as general guidelines for building design.

Variation of amplification factors with wind direction

The measurement results in the previous sections were obtained for wind direction parallel to the passage centerline ($\theta = 0°$). In addition, measurements were made for $\theta = 15°$, 30° and 45° and H = 30 m. Figure 9a shows that for a converging arrangement with w = 10 m, U/U_0 at r = 0 and $(U/U_0)_{max}$ reach a maximum for $\theta = 15°$. This might seem a rather unexpected result, but it resembles the observation by Stathopoulos and Storms (1986) for passages between parallel buildings, where a maximum was found for $\theta = 30°$. Note that this observation is not compromised by the systematic measurement errors discussed earlier. The turbulence intensities at the locations of the maxima are well below 30%, and the "orientation error" due to $\varphi \neq 0°$ actually underestimates U/U_0 for $\theta \neq 0°$. The observation might be attributed to the asymmetry in the corner streams that originate at the corners of the passage at r = 0. Earlier research has shown that the amplification factors in a separate corner stream can be larger than those in the center of the jet that is formed by the interaction of two corner streams (Blocken et al. 2007a). The effect of orientation is somewhat less pronounced for w = 75 m (Fig. 9b).

In general, the variation of U/U_0 with wind direction remains rather limited for the converging arrangement. This might be attributed to the fact that this arrangement "catches" the oncoming wind and tends to direct it to flow along the passage centerline, at least near the location r = 0. Fig. 9c and d for the diverging arrangement on the other hand show a significantly stronger dependence on wind direction, where especially $(U/U_0)_{max}$ decreases rapidly with increasing wind direction.

Discussion of input required for CFD validation

One of the goals of this study was to provide experimental data for the validation of CFD simulations. Some specific features of the flow between converging and diverging building arrangements were observed from the measurements. For further analysis of the flow features, CFD simulations could be used to supplement the present data and to check the hypotheses made, provided that these simulations are carefully validated. Future research will therefore focus on CFD simulation and validation for such passages.

As mentioned earlier, the measurements are inaccurate where turbulence intensities exceed 30%, i.e. upstream and downstream of the passage, but not near the location of most interest (near r = 0). The accuracy is also somewhat less for oblique wind directions. This should be taken into account when comparing these measurement results with numerical data.

Another important aspect towards successful CFD validation is the analysis of the flow in absence of the building models, both experimentally and computationally. Wind tunnel results are generally accompanied by the flow profiles of mean wind speed and turbulence intensity measured in the empty wind tunnel (with roughness elements but without building models present). The location at which these profiles have been measured however is not always specified. Two types of profiles are distinguished (Fig. 10a): (1) the approach flow profiles, which are defined as those measured somewhere upstream of the location where the buildings are to be positioned; and (2) the incident profiles, which are those measured at the location where the buildings will be positioned. It is important that the measurement location is specified, because the approach flow profiles can be quite different from the incident profiles, even at various positions on the turntable, as for example indicated in Fig. 3b for pedestrian-level height. These changes are caused by the development of an internal boundary layer that starts when the set of roughness elements in the wind tunnel ends, and it grows as the flow traverses the turntable.

The computational equivalent of measuring the flow profiles in absence of the building models is performing a CFD simulation in an empty computational domain, i.e. with appropriate roughness settings (Blocken et al. 2007b) but without building models (Fig. 10b). This is important because it is often

wrongfully assumed that the inlet profiles imposed at the domain inlet will remain the same throughout an empty domain. In general, the inlet profiles will be different from the incident profiles, even if the appropriate physical roughness height and roughness constant are specified for the bottom of the computational domain. The main reason for this is the lack of compatibility between the shape of the imposed inlet profiles, the type of turbulence model, the wall functions and other computational parameters (Blocken et al. 2007b). It has been argued that only in exceptional circumstances, both sets of profiles will be identical (Blocken et al. 2007b). Therefore it is important to assess the changes in these profiles, which are also referred to as "unintended streamwise gradients" or "horizontal inhomogeneity", by a simulation in an empty domain. This importance was also stressed earlier by Franke et al. (2004) and demonstrated by CFD simulations by Blocken et al. (2007a, 2007b). In this paper, it is argued that such unintended streamwise gradients should also be assessed in the wind tunnel.

For CFD validation to be successful, it is suggested that the flow conditions in the empty computational domain should be matched to those in the empty wind tunnel, prior to the actual validation exercise with the building models present. It has been shown earlier that not matching these conditions can be detrimental to the success of CFD simulations (Blocken et al. 2007a). Therefore, both the incident flow profiles and the change of the flow over the turntable should be measured and made available for wind tunnel experiments in building aerodynamics.

Conclusions

Wind tunnel measurements of pedestrian wind conditions in passages between converging and diverging building arrangements have been made to provide insight in the related flow patterns, to address some contradictory statements that have appeared in the literature and to provide data for CFD validation. The following conclusions can be made:

- Wind speed amplification factors in diverging passages are often, but not always, larger than in converging passages.
- The maximum wind speed amplification factors in the diverging and converging passages in this study were found to increase monotonically with decreasing passage width-to-height ratio, contrary to some general building design guidelines proposed in the past for such building configurations.
- The maximum wind speed amplification factor in the diverging passage occurs for wind direction $\theta = 0°$ (i.e. parallel to the passage centerline), while the maximum value for the converging passage is found for $\theta = 15°$.
- This study was limited to configurations of two long narrow perpendicular buildings with fixed and identical dimensions and was conducted with given incident flow profiles. As a result, further research is needed to expand the validity of the present findings.
- To provide sufficient information for CFD validation based on these data, the measured incident flow profiles and also the change of the approach flow over the empty wind tunnel turntable have been measured and reported. These are important features that need to be matched in a CFD simulation of the flow in an empty computational domain, prior to the actual validation exercise with the building models present.

Acknowledgements

The authors would like to thank Ms. Panagiota Karava and Mr. Amit Gupta, PhD students at the Building Aerodynamics Laboratory of Concordia University, for their kind assistance during the wind tunnel tests.

Notation

The following symbols are used in this paper

B = building width

H = building height
I = turbulence intensity
I_0 = turbulence intensity at pedestrian height without buildings present
L = building length
U = mean wind speed
U_0 = mean wind speed at pedestrian height without buildings present
U_g = mean wind speed at gradient height
Re_b = building Reynolds number
r = dimensionless coordinate along passage centerline
w = passage width
α = power law exponent
θ = wind direction, relative to passage centerline
φ = angle between local wind direction and normal to hot wire, in a horizontal plane

References

ASCE (2003). Aerodynamics Committee. *Outdoor human comfort and its assessment*, State of the Art Report, Task Committee on Outdoor Human Comfort, American Society of Civil Engineers, Boston, VA, USA.

Beranek, W. J. (1982). *Beperken van windhinder om gebouwen*, deel 2, Stichting Bouwresearch no. 90, Kluwer Technische Boeken BV, Deventer, The Netherlands, 149 p + 89 p, (in Dutch).

Blocken, B., and Carmeliet, J. (2004). "A review of wind-driven rain research in building science." *J. Wind Eng. Ind. Aerodyn.,* 92(13), 1079-1130.

Blocken, B., Roels, S., and Carmeliet, J. (2004). "Modification of pedestrian wind comfort in the Silvertop Tower passages by an automatic control system." *J. Wind Eng. Ind. Aerodyn.*, 92(10), 849-873.

Blocken, B., and Carmeliet, J. (2006). "The influence of the wind-blocking effect by a building on its wind-driven rain exposure." *J. Wind Eng. Ind. Aerodyn.*, 94(2), 101-127.

Blocken, B., Carmeliet, J., and Stathopoulos, T. (2007a). "CFD evaluation of wind speed conditions in passages between parallel buildings – effect of wall-function roughness modifications for the atmospheric boundary layer flow." *J. Wind Eng. Ind. Aerodyn.*, 95(9-11), 941-962.

Blocken, B., Stathopoulos, T., and Carmeliet, J. (2007b). "CFD simulation of the atmospheric boundary layer: wall function problems." *Atmos. Environ.*, 41(2), 238-252.

Bottema, M. (1993). *Wind climate and urban geometry*, PhD thesis. Building Physics Group, Technical University of Eindhoven, The Netherlands.

Cook, N.J., and Redfearn, D. (1976). "Calibration and use of a hot-wire probe for highly turbulent and reversing flows." *J. Wind Eng. Ind. Aerodyn.*, 1(3): 221-231.

Franke, J., Hirsch, C., Jensen, A.G., Krüs, H.W., Schatzmann, M., Westbury, P.S., Miles, S.D., Wisse, J.A., and Wright, N.G. (2004). "Recommendations on the use of CFD in wind engineering, in: proceedings of the International Conference on Urban Wind Engineering and Building Aerodynamics", (Ed. van Beeck JPAJ), *COST Action C14, Impact of Wind and Storm on City Life Built Environment*, von Karman Institute, Sint-Genesius-Rode, Belgium, 5 - 7 May 2004.

Gandemer, J. (1975). "Wind environment around buildings: aerodynamic concepts." *Proc., 4th Int. Conf. Wind Effects on Buildings and Structures*, Heathrow 1975, Cambridge University Press, 423-432.

Ishizaki, H., and Sung, I. W. (1971). "Influence of adjacent buildings to wind." *Proc. 3rd Int. Conf. Wind Effects on Buildings and Structures*, Tokyo 1971, Japan, I.15-1-I.15-8.

Lawson, T. V. (1980). *Wind effects on buildings*, Vol. 1, Applied Science Publishers Ltd., London, England.

Malla R.B., Binienda W.K., and Maji, A.K. (2006). *Earth & Space 2006. Engineering, Construction and Operations in Challenging Environments*. Proc. 10th Biennial Int. Conf. on Engineering, Construction and Operations in Challenging Environments, League City/Houston, TX, March 5-8.

Meroney, R.N. (2004). “Wind tunnel and numerical simulation of pollution dispersion: a hybrid approach.” Working paper, Croucher Advanced Study Insitute on Wind Tunnel Modeling, Hong Kong University of Science and Technology, 6-10 December, 2004, 60 pp.

Snyder, W.H. (1981). *Guideline for fluid modeling of atmospheric diffusion*. U.S. Environmental Protection Agency Report No. EPA-600/8-81-009.

Stathopoulos, T. (1984). “Design and fabrication of a wind tunnel for building aerodynamics.” *J. Wind Eng. Ind. Aerodyn.*, 16, 361-376.

Stathopoulos, T., and Storms, R. (1986). “Wind environmental conditions in passages between buildings.” *J. Wind Eng. Ind. Aerodyn.*, 24, 19-31.

Stathopoulos, T., Wu, H., and Bédard, C. (1992). “Wind environment around buildings: a knowledge-based approach.” *J. Wind Eng. Ind. Aerodyn.*, 41-44, 2377-2388.

Stathopoulos, T., and Wu, H. (1995). “Generic models for pedestrian-level winds in built-up regions.” *J. Wind Eng. Ind. Aerodyn.*, 54-55, 515-525.

Stathopoulos, T. (2002). “The numerical wind tunnel for industrial aerodynamics: Real or virtual in the new millennium?” *Wind Struct.*, 5(2-4), 193-208.

Stathopoulos, T. (2006). “Pedestrian-level winds and outdoor human comfort.” *J. Wind Eng. Ind. Aerodyn.*, 94(11), 769–780.

To, A.P., and Lam, K. M. (1995). “Evaluation of pedestrian-level wind environment around a row of tall buildings using a quartile-level wind speed descriptor.” *J. Wind Eng. Ind. Aerodyn.*, 54-55, 527-541.

Wiren, B.G. (1975). “A wind tunnel study of wind velocities in passages between and through buildings.” *Proc. 4th Int. Conf. Wind Effects on Buildings and Structures*, Heathrow 1975, Cambridge University Press, 465-475.

FIGURE CAPTIONS

Figure 1. Top view of three types of passages between buildings.

Figure 2. Building configuration (top view), building dimensions and dimensionless coordinate r for (a) converging and (b) diverging arrangement

Figure 3. (a) Incident flow profiles of mean wind speed ratio (bottom axis) and turbulence intensity (top axis) at r = 0. (b) Pedestrian-level flow change of the ratios U/U_0 and I/I_0 in streamwise direction over part of the turntable.

Figure 4. U/U_0 and I/I_0 along passage centerline for the converging building arrangement with H = 30 m.

Figure 5. U/U_0 and I/I_0 along passage centerline for the converging building arrangement with H = 60 m.

Figure 6. U/U_0 and I/I_0 along passage centerline for the diverging building arrangement with H = 30 m.

Figure 7. U/U_0 and I/I_0 along passage centerline for the diverging building arrangement with H = 60 m.

Figure 8. U/U_0 as a function of w/H for four building configurations (converging, diverging, H = 30 m and H = 60 m). (a) U/U_0 at location r = 0. (b) Maximum value of U/U_0 on passage centerline between r = -1 and r = 1.

Figure 9. Influence of wind direction on U/U_0 at r = 0 and on $(U/U_0)_{max}$ for (a) converging passage with w = 10 m and (b) w = 75 m; (c) diverging passage with w = 10 m and (d) w = 75 m. H = 30 m for all cases.

Figure 10. Schematic representation of (a) empty wind tunnel and (b) empty computational domain in which the incident flow conditions and flow change over the “turntable” have to be matched.

Figures

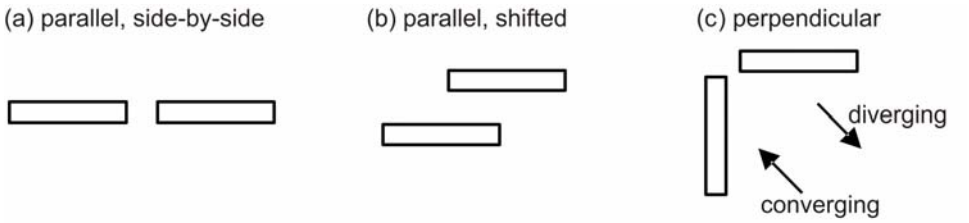

Figure 1. Top view of three types of passages between buildings.

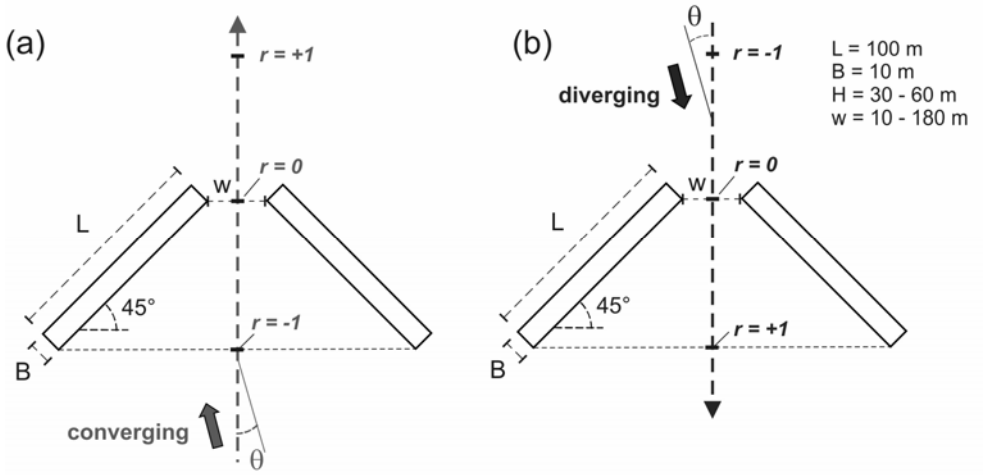

Figure 2. Building configuration (top view), building dimensions and dimensionless coordinate r for (a) converging and (b) diverging arrangement

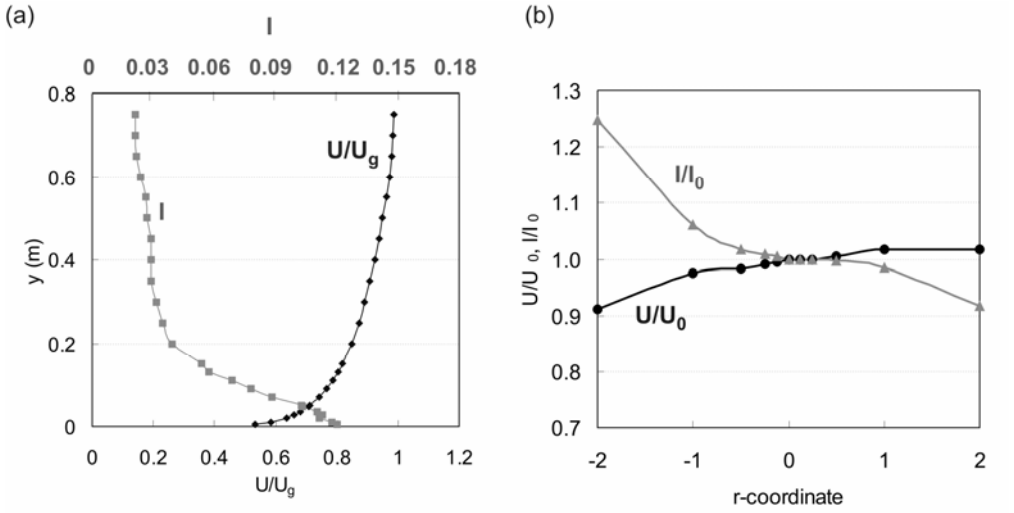

Figure 3. (a) Incident flow profiles of mean wind speed ratio (bottom axis) and turbulence intensity (top axis) at r = 0. (b) Pedestrian-level flow change of the ratios U/U_0 and I/I_0 in streamwise direction over part of the turntable.

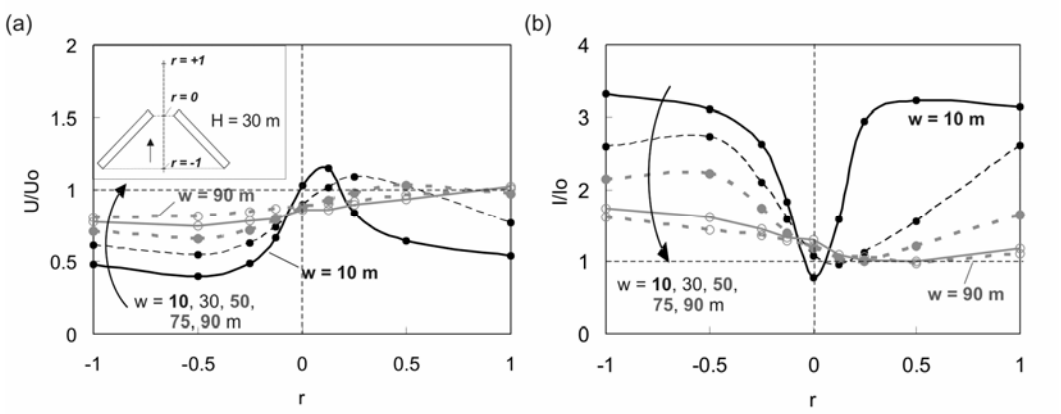

Figure 4. U/U_0 and I/I_0 along passage centerline for the converging building arrangement with H = 30 m.

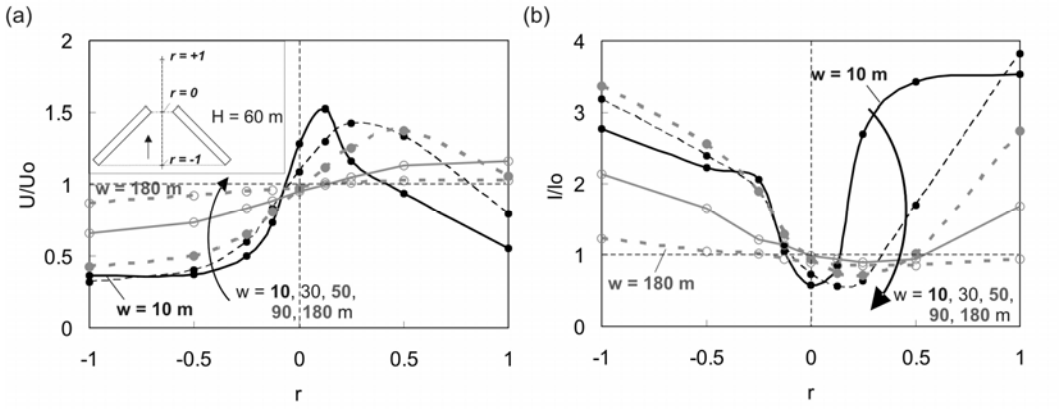

Figure 5. U/U_0 and I/I_0 along passage centerline for the converging building arrangement with H = 60 m.

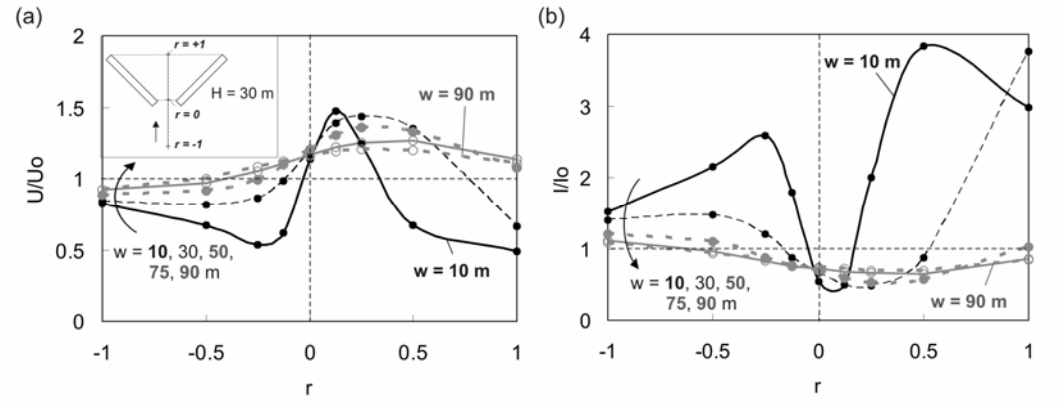

Figure 6. U/U_0 and I/I_0 along passage centerline for the diverging building arrangement with H = 30 m.

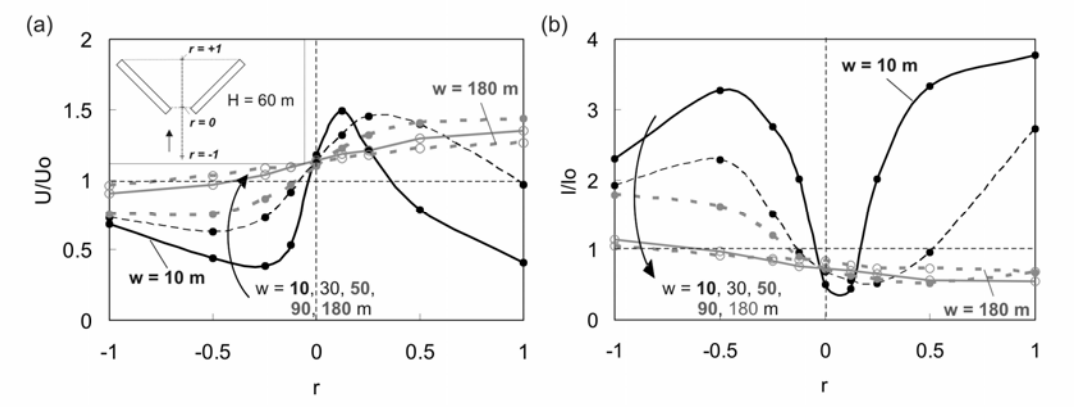

Figure 7. U/U_0 and I/I_0 along passage centerline for the diverging building arrangement with H = 60 m.

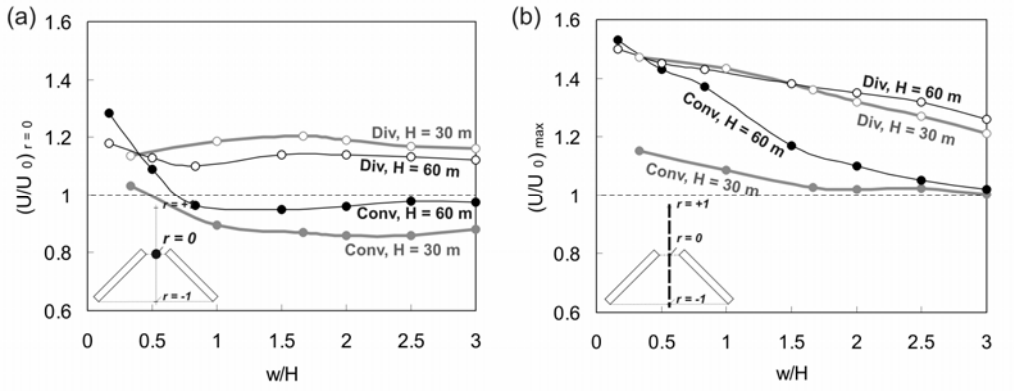

Figure 8. U/U_0 as a function of w/H for four building configurations (converging, diverging, H = 30 m and H = 60 m). (a) U/U_0 at location r = 0. (b) Maximum value of U/U_0 on passage centerline between r = -1 and r = 1.

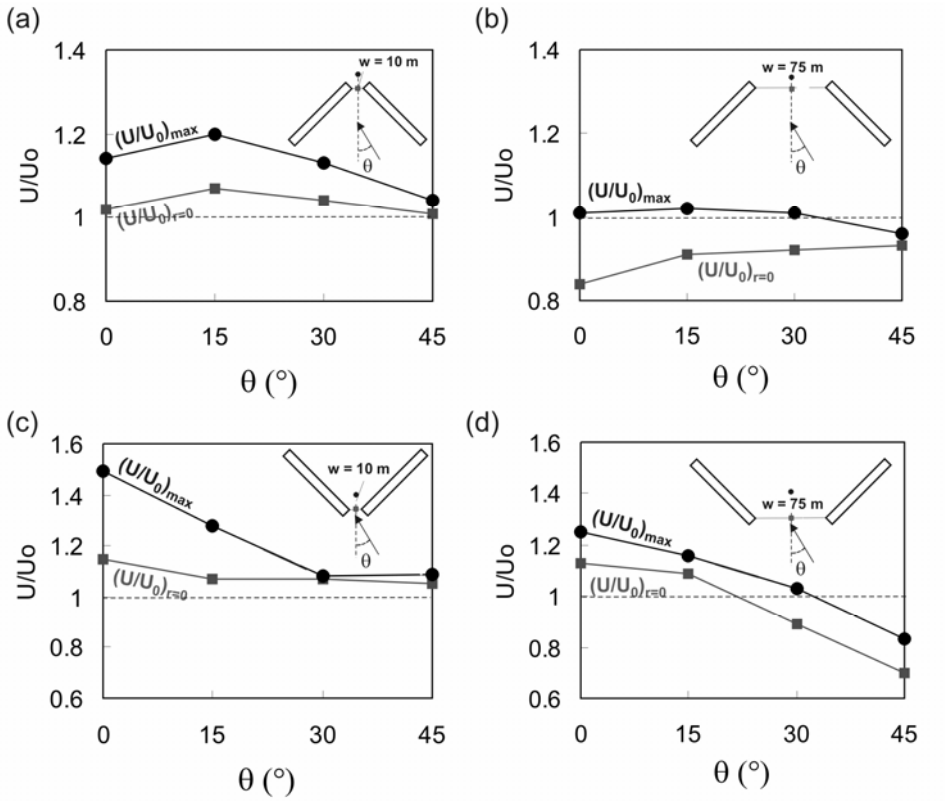

Figure 9. Influence of wind direction on U/U_0 at r = 0 and on $(U/U_0)_{max}$ for (a) converging passage with w = 10 m and (b) w = 75 m; (c) diverging passage with w = 10 m and (d) w = 75 m. H = 30 m for all cases.

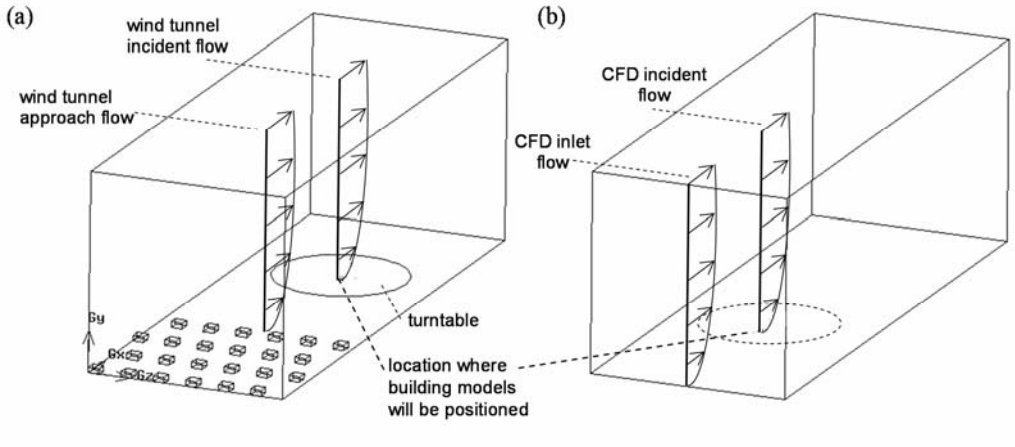

Figure 10. Schematic representation of (a) empty wind tunnel and (b) empty computational domain in which the incident flow conditions and flow change over the "turntable" have to be matched.